(Ru-)Mo_2C (MXene) catalysts for ammonia synthesis: From Haber-Bosch to chemical looping processes

Charlotte Croisé, Xavier Courtois, Stéphane Célérier, Lola Loupias, Christine Canaff, Julie Rousseau, Nicolas Bion, Fabien Can

Materials Today Catalysis 7 (2024) 100066

Contents lists available at ScienceDirect

Materials Today Catalysis

journal homepage: www.journals.elsevier.com/materials-today-catalysis

(Ru-)Mo_2C (MXene) catalysts for ammonia synthesis: From Haber-Bosch to chemical looping processes

Charlotte Croisé, Xavier Courtois *, Stéphane Célérier *, Lola Loupias, Christine Canaff, Julie Rousseau, Nicolas Bion, Fabien Can

Institut de Chimie des Milieux et Matériaux de Poitiers (IC2MP), Université de Poitiers, CNRS, 4 rue Michel Brunet TSA 51106 86073 Poitiers Cedex 9, France

ARTICLE INFO

Keywords:
Mo_2CT_x MXene
Ammonia synthesis
Haber-Bosch process
Chemical looping
Molybdenum nitride

ABSTRACT

This study investigated (Ru-)Mo_2C (MXene) materials for ammonia thermo-catalytic synthesis under atmospheric or moderate pressure. Under a H_2-N_2 (3:1) flow, the Mo_2C MXene phase showed limited activity in ammonia synthesis at atmospheric pressure at 400 °C (0.01 mmol h^{-1} g^{-1}), which increased significantly with temperature and pressure, reaching 2.07 mmol h^{-1} g^{-1} at 500°C and under 5 bar. Interestingly, Mo-based MXene was able to generate an appreciable quantity of ammonia without promoters such as ruthenium, the most active metal for the ammonia synthesis reaction. Unexpectedly, the addition of Ru to Mo_2C did not enhance its activity. The nitriding of the MXene under NH_3 or N_2 was then performed and characterized. A thermal treatment under NH_3 (600 °C, 5 bar) was efficient and, interestingly, nitriding also occurred in a lower extent under N_2 (600 °C, 5 bar) for the sample containing ruthenium. The N-containing MXene produced ammonia under pure H_2 flow from temperatures lower than 250 °C. Consecutive nitriding treatments and ammonia production under pure H_2 were successfully achieved and demonstrated for 5 cycles. This result is promising for chemical looping ammonia production process. This work highlights essential aspects that should be explored for future advances to consider using Mo_2CT_x MXene for the efficient thermal production of ammonia.

1. Introduction

Ammonia is one of the most synthesized chemical compounds in the world, with a production of about 180 million tons per year, in continuous expansion [1]. Ammonia is used in many industrial sectors, in particular for soil fertilization [2]. Ammonia has also been identified as a promising carbon free fuel for power generation and energy carrier, particularly attractive as a hydrogen storage molecule [3].

The well-known Haber-Bosch (HB) process for ammonia synthesis ($N_2 + 3\,H_2 \leftrightarrows 2NH_3$) usually involves an iron-based catalyst that requires high reaction temperatures (400–600 °C) and high pressures (150–200 bar) [4]. This technology, including hydrogen production, is responsible for 1–2 % of the world's annual energy consumption and more than 1 % of total annual global emissions of anthropogenic CO_2 [4,5]. More efficient ammonia production requires less energy-consuming conditions, which remains a major challenge, according to the ammonia roadmap technology [6]. To achieve this objective, the development of new catalytic materials, active at lower temperatures and pressures, retains particular attention. Over the last decades, with the aim to promote the N_2 activation molecule and avoid the hydrogen poisoning effect, several new heterogeneous catalyst families have been proposed, such as hydrides, electrides, or nitrides, generally associated with ruthenium [7]. Among the large variety of studied material families, electronic conductors are especially attractive since the electronic enrichment of the antibonding orbitals of N_2 is necessary to weaken the very stable N≡N triple bond and promote N_2 activation [8]. In this context, the properties of two-dimensional (2D) materials such as MXenes appear attractive, especially associated with Ru nanoparticles (NPs) to make a co-catalyst, as demonstrated theoretically [9,10]. This class of 2D materials follows the formulae $M_{n+1}X_nT_x$ and is composed of $M_{n+1}X_n$ lamellae, where M is an early transition metal (TM) such as Ti, Cr, V, Mo and/or Nb; X is carbon or nitrogen with n ranging mainly from 1 to 4; and T stands for terminal groups grafted to the surface [11]. MXenes have gained increasing attention for a large range of applications since their first report in 2011 [12]. The combination of the layered 2D structure with numerous MXene compositions offers excellent physicochemical properties such as high thermal and electronic conductivity, high Young modulus, tuneable electronic band gap, optical

* Corresponding authors.
E-mail addresses: xavier.courtois@univ-poitiers.fr (X. Courtois), stephane.celerier@univ-poitiers.fr (S. Célérier).

https://doi.org/10.1016/j.mtcata.2024.100066
Received 21 May 2024; Received in revised form 13 September 2024; Accepted 19 September 2024
Available online 23 September 2024

transparency or hydrophilic surface, among other [11]. Recently, they have also been increasingly studied in heterogeneous catalysis, particularly Mo_2CT_x [13–19].

Two recent DFT studies on various M_2X MXene materials (M = Mo, Ta, Ti, W; X = C, N) highlighted interesting behaviour toward nitrogen activation. First, Shao *et al.* [20] concluded that Mo_2C and W_2C should dissociate easily N_2 with strong charge transfer, most of the steps being exothermic. Secondly, Gouveia *et al.* [10] showed that the N_2 adsorption on carbide or nitride-based MXene is associated with an elongation of the N≡N bond by approximately 20 % (1.35 Å vs 1.11 Å for gaseous N_2), which should promote the N_2 dissociation. In this study, W_2N shows the best performances for the N_2 dissociation among the studied MXenes. Additionally, Lopez *et al.* [21] showed that pristine MXenes, especially 2D-Mo_2C, can be promising hydrogenation catalysts. Along with nitrogen dissociation, this is also a key step in the Haber-Bosch process. To our knowledge, despite those interesting theoretical results, experimental studies of MXenes for the thermocatalytic ammonia synthesis have not been reported yet. In contrast, MXene materials are largely studied for ammonia electrosynthesis, especially since the publication of Luo *et al.* [22] which showed the attractive performance of $Ti_3C_2T_x$ materials in N_2 electro-reduction. Unlike the HB process, the ammonia electrosynthesis could be performed at room temperature. However, despite numerous studies involving various MXenes (Mo_2C, Ti_3C_2, Mo_2TiC_2) [23–27], with the addition of ruthenium, copper, or iron [28–30], the observed ammonia yields remain notably low or even questionable and prohibitively far from the yield obtained in the industrial HB process.

Additionally, the nitride form of Mo-MXene, *i.e.* Mo_2NT_x, could be an excellent candidate for the thermal ammonia synthesis [10], not only for its predicted ability for N_2 dissociation mentioned above, but also to serve as a source of nitrogen. This opens new prospects for the chemical looping ammonia synthesis process, a promising alternative to the HB process to reduce its energy demand [31]. The chemical looping process is divided into two sub-reactions in which N_2 and H_2 reactants are fed separately with (i) the feeding N_2 (charge step) and (ii) the feeding H_2 (discharge step, ammonia production), operated in optimized conditions (flow rate, temperature, pressure). This process avoids the competitive adsorption of N_2 and H_2 and does not suffer from the kinetic and thermodynamic limitations of the HB process. A thermal treatment of Mo_2CT_x under NH_3 is a known nitriding route to Mo_2NT_x [32].

The aim of this work is to determine the potential of Mo_2CT_x MXene as catalyst for the HB ammonia synthesis in the 400–500 °C temperature range, under moderate pressure (1–5 bar). The behaviour of this MXene toward N_2 and NH_3 is also examined in terms of nitride formation and the reactivity of the resulting material toward H_2 is investigated. Finally, nitriding/hydrogenation cycles to mimic a chemical looping process are studied. The influence of the impregnation of ruthenium on the MXene for the HB process and the nitriding process is also explored. Overall, this study highlights novel aspects that should be explored in future works to enable the use of Mo_2CT_x MXene for the energy-efficient thermal production of ammonia.

2. Materials and methods

2.1. Syntheses of materials

2.1.1. Mo_2Ga_2C phase (MAX-like phase)

The synthesis of Mo_2Ga_2C (MAX-like phase) was performed as described by Benchakar *et al.* [33]. Desired masses of molybdenum carbide β-Mo_2C (99.5 %, Alfa Aesar) and gallium (Magnametals, 99.99 %), corresponding to a 1:8 molar ratio, were crushed together in a mortar to obtain a homogeneous paste. The paste was then transferred into a vacuum glass tube and then thermally treated at 850 °C for 170 h (heating rate: 5 °C min^{-1}). The resulting powder was treated with hydrochloric acid (35 %, VWR) for one night under magnetic stirring to remove the excess of gallium. The solid was washed with ultrapure water (MilliQ®, Millipore) until reaching a pH close to 5. After filtration, the resulting powder was dried at room temperature in a desiccator. Finally, the powder was sieved in order to select grain sizes lower than 25 μm. The resulting sample is denoted Mo_2Ga_2C.

2.1.2. Mo_2C MXene phase

The multilayer Mo_2CT_x MXene phase was obtained from Mo_2Ga_2C by etching of gallium (Ga) using a modified procedure reported in [13]. 40 mL of a HF solution (Sigma Aldrich, 48 %) was added in a PTFE tube with 1 g of the Mo_2Ga_2C powder. The mixture was homogenized in an ultrasonic bath for 15 min and then placed in an autoclave for 24 h at 160 °C. The suspension was then washed with ultrapure water and centrifuged several times until the pH value of the supernatant solution reached 5 (3500 rpm, corresponding to 1575 g – rotor F-34–6–38, Eppendorf centrifuge 5804). The resulting powder was then recovered by filtration under vacuum, dried in a desiccator under air and at atmospheric pressure, and stored in a glove box under argon. The resulting Mo_2CT_x MXene is denoted Mo_2C for brevity.

2.1.3. Ruthenium impregnation

Ruthenium was added by wet impregnation from a commercial Ru $(NO)(NO_3)_3$ solution (Alfa Aesar, 1.5 % w/v). The desired amount of ruthenium precursor to reach a final theoretical content of 2.5 wt% was diluted in 5 mL ultrapure water, and mixed with 400 mg of Mo_2C. After one night under stirring, the water was evaporated at 80 °C and, the resulting powder was dried at 100 °C for one night in a drying oven. The sample was then treated under a pure H_2 flow (60 mL min^{-1}) at 400 °C for 4 h (heating rate: 5 °C.min^{-1}) to form the metallic ruthenium. The resulting sample is denoted Ru/Mo_2C.

2.1.4. Nitriding treatment

Several nitriding methods have been investigated for Mo_2C and Ru/Mo_2C samples. First, the nitriding technique based on the work of Urbankowski *et al.* [32] involved a thermal treatment at 600 °C and 5 bar for 5 h under a 25 % NH_3 −75 % He mixture (total flow rate: 10 mL min^{-1}). The samples are then denoted Mo_2C_{NH3} and Ru/Mo_2C_{NH3}. Nitriding under N_2 was also examined (600 °C, 5 bar, 5 h; N_2 flow rate: 60 mL min^{-1}), samples are then denoted Mo_2C_{N2} and Ru/Mo_2C_{N2}. Note that a purge under argon was performed at 600 °C at the end of the NH_3 or N_2 treatment to desorb the reactant molecules from the surface of the material.

The possible nitriding during catalytic tests under $N_2 + H_2$ flow (400 °C to 500 °C, from 1 to 5 bar) was also examined. The notation of the corresponding samples after the catalytic tests is Mo_2C_{test} and Ru/Mo_2C_{test}.

2.2. Characterization techniques

The morphology of synthesized materials was analysed by scanning electron microscopy (SEM) using a MEB-FEG JSM-7009 F microscope (JEOL Company) with a maximal resolution of 0.7 nm. This apparatus is equipped with a field emission gun and an energy dispersive X-ray spectrometer (EDX) 6/30 (Brücker) for the determination and mapping of chemical elements.

The sample structure and the metal dispersion were investigated by transmission electron microscopy (JEOL 2100 LaB6, 200 kV). For grid preparation, the sample was ultrasonicated in ethanol, and a drop of the upper suspension was deposited on the grid.

X-Ray diffraction measurements were performed at room temperature from 2θ = 3° to 2θ = 70°, with a step interval of 0.066 ° and an acquisition time of 420 s per step (EMPYREAN PANalytical diffractometer in Bragg-Brentano configuration and equipped with a copper anode source, CuK_α =0.15406 nm). An ultra-fast X-Ray detector (X'Celerator) was used to collect the signals. The diffractograms were processed with the HighScorePlus® software.

The Mo, Ga, and Ru content of the prepared materials were

determined by Inductively Coupled Plasma-Optical Emission Spectrometry (ICP-OES) using a PerkinElmer Optima 2000DV instrument.

Additionally, elemental carbon and nitrogen contents were assessed using a Thermoquest NA 2100 analyser. The sample was *in situ* treated under oxygen at 1020 °C, and gaseous effluents were analysed *via* a gas chromatography column associated with a thermal conductivity detector.

The XPS analyses were carried out with a Kratos Axis Ultra DLD spectrometer using a monochromatic Al K_α source (1486.6 eV, 10 mA, 15 kV). Instrument base pressure was 9×10^{-8} Pa. High-resolution spectra were recorded using an analysis area of 300 μm × 700 μm and a 20 eV pass energy, corresponding to a Ag $3d_{5/2}$ full width at half maximum (FWHM) of 0.55 eV. Data were acquired with 0.1 eV steps. All spectra presented in this work have their binding energy scale calibrated against the Fermi edge. For the curve fittings, a Shirley background model was used. Lorentzian asymmetric functions (LA) were selected for the contributions related to the MXenes, whereas Gaussian/Lorentzian symmetric functions (GL) were selected for oxides and impurities. Indeed, asymmetric functions are required for curve fittings of electronic conducting materials such as MXenes [34]. The XPS spectra were then processed using CasaXPS software. The samples were exposed to air for less than 30 min before XPS analyses (including transfer from catalytic reactor to glove box under argon and from the glove box to the XPS chamber).

2.3. Catalytic tests

The ammonia synthesis activity measurement was carried out in a fixed-bed reactor. A stoichiometric H_2:N_2 gas mixture (3:1 ratio; gas purity > 99.9999 %; total flow rate of 60 mL min^{-1}) was supplied by electronic mass-flow controllers. The catalyst (100 mg, sieved fraction between 40 and 100 μm) was placed in a home-made pressure reactor equipped with a back-pressure regulator (Bronkhorst). The outlet ammonia concentration was continuously monitored (1 Hz) by a MKS 2030 Multigas infrared analyser with a high NH_3 sensitivity (2–3 ppm). The ammonia production was measured during isotherms at 400 °C, 450 °C and 500 °C (heating rate: 5 °C min^{-1}). For each tested temperature, three consecutive working pressures were applied (1, 3, and 5 bar, one hour each). Results are presented as ammonia concentration in the effluent (ppm) or ammonia synthesis rate (mmol h^{-1} g^{-1}). Note that a rate of 1.0 mmol h^{-1} g^{-1} corresponds to an outlet ammonia concentration of 670 ppm.

3. Results and discussion

3.1. Characterization of the synthesized samples

The morphologies of the MAX and MXene phases were observed by scanning electron microscopy. The SEM images reported in Fig. 1 indicate that the MAX phase structure exhibits a "tile" type morphology. The microstructure of the resulting Mo_2CT_x (denoted Mo_2C) is characteristic of a multi-layers MXene, with oriented layers stacked in the grain [35], in contrast to delaminated MXene obtained using a delamination step in TBAOH leading to the formation of a film [36].

The diffractograms of Mo_2Ga_2C and Mo_2C materials are presented in Fig. 2. The removal of the gallium layer during the exfoliation step involves a shift of the (002) peak of the initial MAX phase (c = 18.1 Å) towards lower diffraction angles (9.8–8.6 ° for 2θ), leading to a higher value of the c lattice parameter for the corresponding MXene (c = 20.5 Å). This is due to the grafting of terminal groups (O, OH, and F) at the surface of the MXene layer and to the insertion of a water layer in the interlayer space [36,37]. However, as evidenced by the peak at $2\theta = 9°$ in the XRD pattern of the MXene, the etching of Ga is incomplete even if the amount of the remaining MAX phase seems low. According to this observation, ICP-OES analysis indicates that 16 % of the initial gallium remain in the solid related to the Mo content (Table 1). Thus, considering $Mo_2Ga_{1.9}C$ as the composition of the precursor, the Mo_2C sample is composed of 84 mol% of MXene and 16 mol% of remaining MAX phase. Taking into account the carbon elemental analysis (Table 1), the obtained Mo/C ratio is close to 2.2. This value is consistent with the

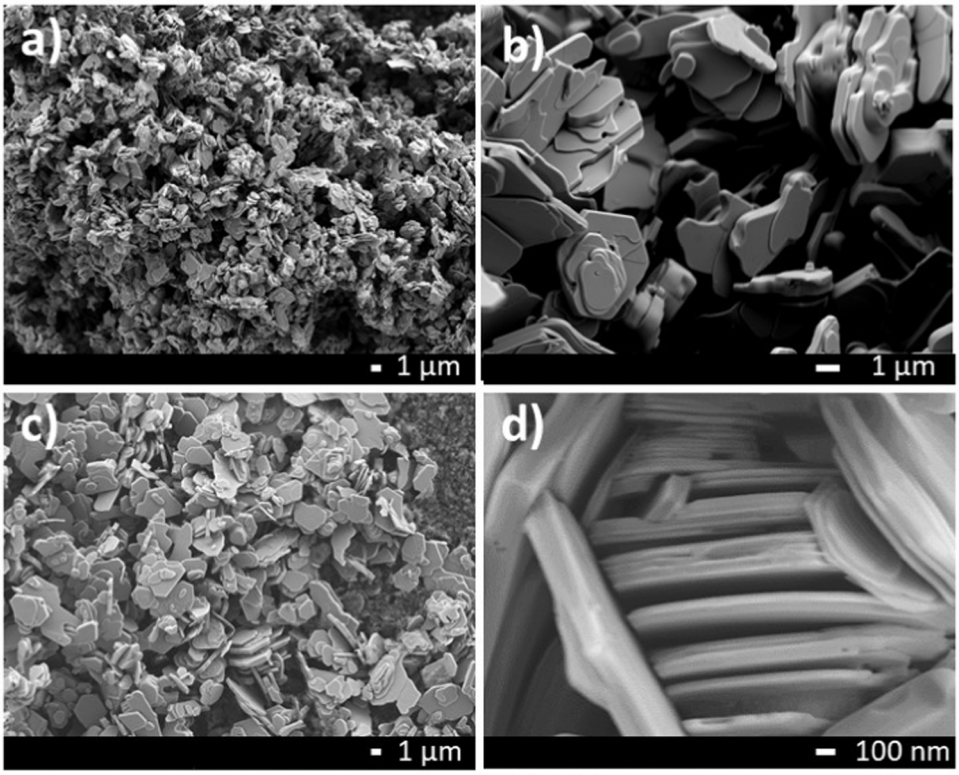

Fig. 1. Scanning electron microscopy images of Mo_2Ga_2C (a and b) and Mo_2C (c and d) samples.

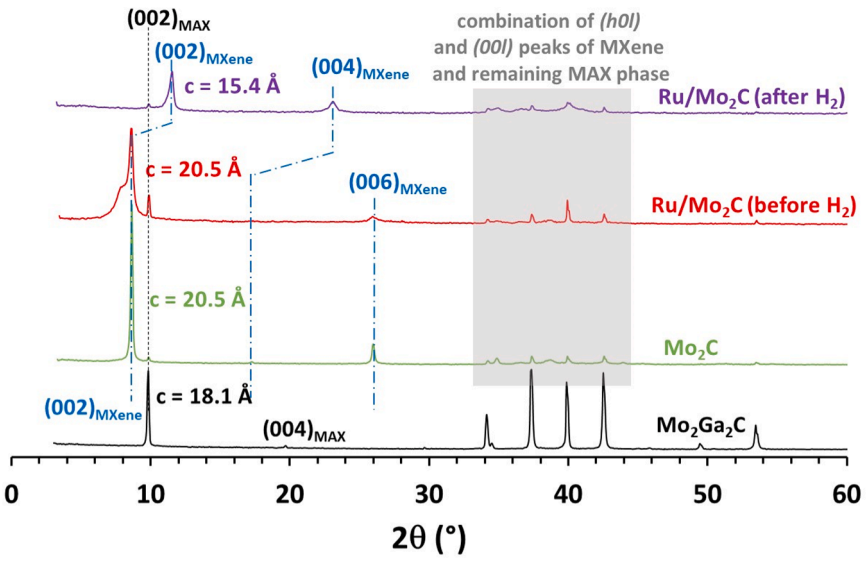

Fig. 2. XRD patterns of Mo_2Ga_2C, Mo_2C, and Ru/Mo_2C before and after thermal treatment under H_2.

Table 1
Mo_2C, Ru/Mo_2C and Mo_2Ga_2C composition from ICP and CHNS analyses. The obtained formulation is normalized for 2 Mo. The wt% is reported in bracket.

sample	Chemical formulae normalized for Mo2			
	Mo	Ga	C	Ru
Mo_2Ga_2C	2.00 (53.5)	1.90 (36.1)	0.89 (3.0)	0.00 (0)
Mo_2C	2.00 (78.4)	0.30 (8.5)	0.91 (4.4)	0.00 (0)
Ru/Mo_2C	2.00 (70.2)	0.29 (7.3)	0.82 (3.6)	0.05 (2.2)

theoretical ratio for Mo_2C, although a slight carbon sub-stoichiometry is observed.

After ruthenium impregnation and the drying step at 100 °C, the diffractogram of the Ru/Mo_2C sample exhibits the same (002) peak position compared to the host Mo_2C material (Fig. 2). However, a shoulder is observed at a lower angle, characteristic of an interstratification phenomenon [38], indicating a possible inhomogeneous insertion of Ru^{3+} cation between the layers. Nonetheless, this insertion is probably limited because ruthenium is found on the surface of the multi-layer MXene after H_2 reduction, as discussed below, relying on the TEM analysis. After the thermal treatment at 400 °C for 4 h under hydrogen, the diffractogram of Ru/Mo_2C (Fig. 2) shows a shift of the (002) peak towards higher angles (2θ = 11.5°). The corresponding c lattice parameter is then 15.4 Å, which is smaller than that of Mo_2C (20.5 Å) and Mo_2Ga_2C MAX phase (18.1 Å). This change is attributed to the removal of water in the MXene interlayer spacing during the thermal treatment under H_2 at 400 °C. ICP-OES analysis shows that ruthenium deposition and the thermal treatment under H_2 induce a limited impact on the MXene composition (Table 1), although the carbon content seems to decrease slightly. This could be explained by a partial carbon removal in Mo_2CT_x, as previously observed by Kountoupi *et al.* [19] under pure H_2 treatment at 500 °C. The elemental analysis also indicates that the ruthenium content is 2.2 wt%, close to the targeted loading of 2.5 wt%. Additionally, Ru/Mo_2C sample was also analysed by TEM (Fig. 3). Ruthenium nanoparticles of 2–3 nm are observed at the surface of the multi-layer MXene. This particle size is commonly considered as suitable for the ammonia synthesis reaction due to the formation of B_5-type active sites [39]. However, the particles are highly agglomerated, indicating a low degree of Ru accessibility. The selected area electron diffraction (SAED) of the nanoparticles confirms the formation of metallic ruthenium with d_{101} = 2.0 Å and d_{100} = 2.3 Å (JCPDS file n°00–001–1256: d_{101} = 2.04 Å and d_{100} = 2.32 Å).

Mo_2C and Ru/Mo_2C were also analysed by XPS. Experimental and fitted curves are reported in Fig. 4 and Tables S2 and S3 for Mo 3d, C 1 s, and Ru 3d regions. Complementary analysis for O 1 s and F 1 s regions are shown in Figure S1, Tables S2 and S3.

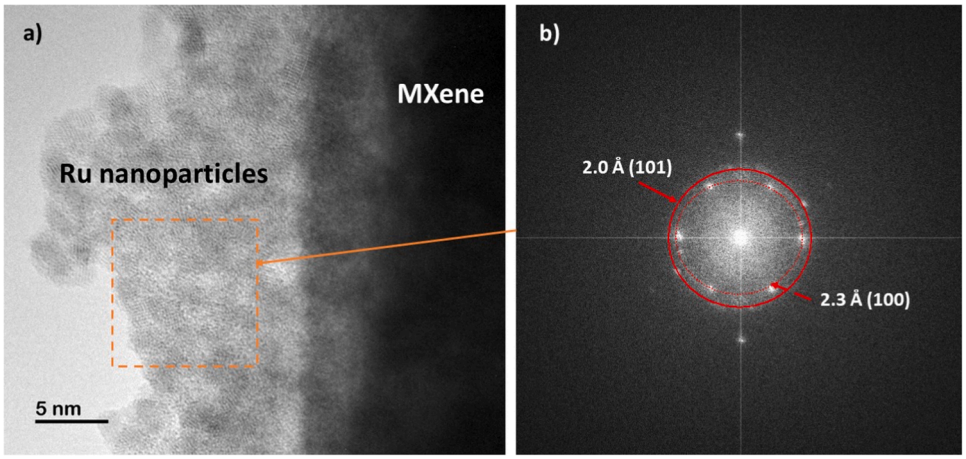

Fig. 3. Representative TEM image of Ru/Mo_2C (a); SAED pattern obtained for Ru nanoparticles (b).

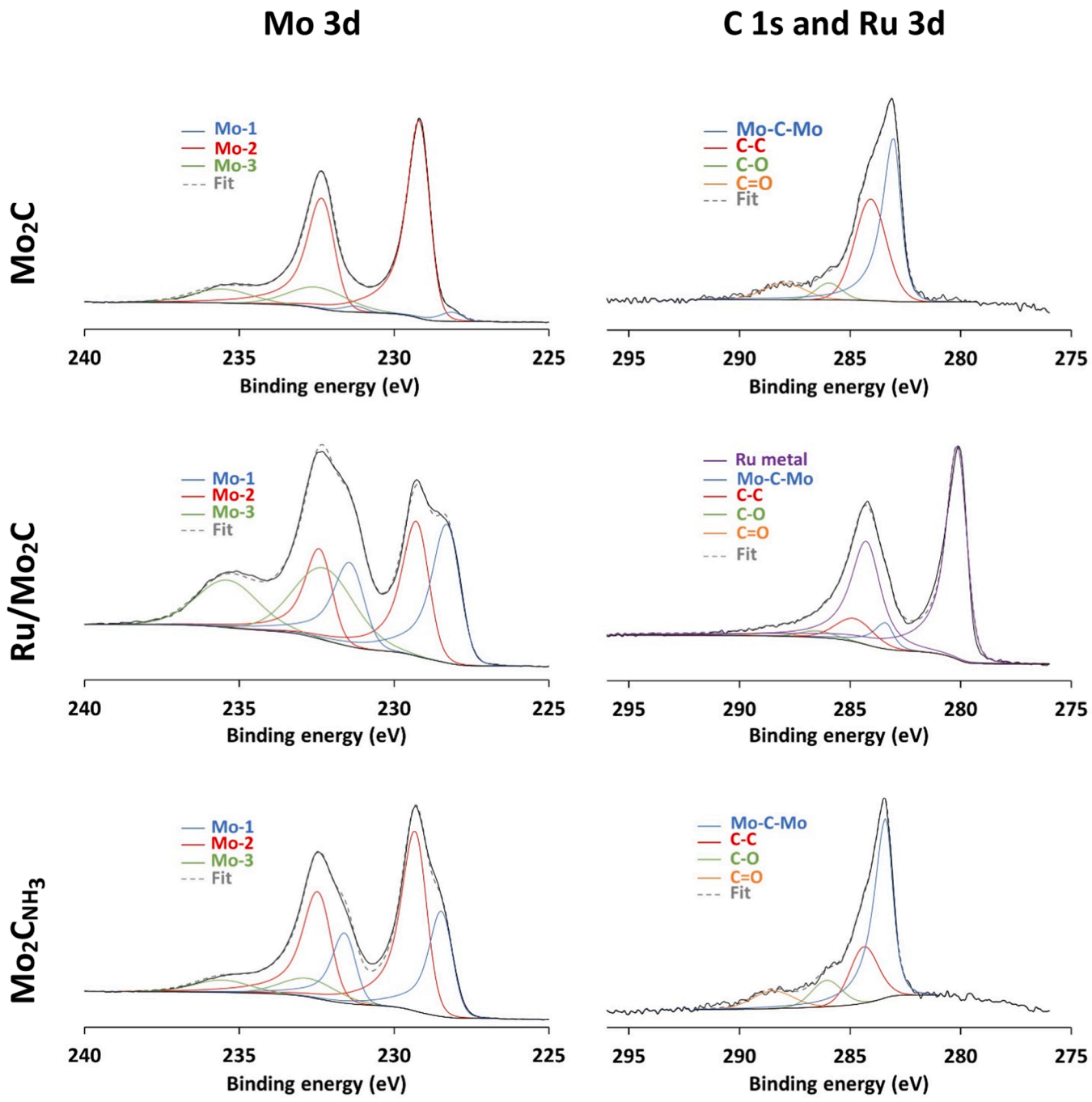

Fig. 4. High resolution XPS spectra with curve fitting of Mo 3d, C 1 s, and Ru 3d regions recorded on Mo_2C, Ru/Mo_2C, and Mo_2C_{NH3}. All spectra are normalized to the most intense peak for each region (color printing required).

In the Mo 3d region, as expected, several doublets ($3d_{5/2}$ and $3d_{3/2}$) are observed, which is due to spin-orbit coupling. For simplicity, the following discussion is based only on the lowest energy photopeak ($3d_{5/2}$, between 228 and 233 eV). Three contributions were used for the spectral decomposition in this region, labelled Mo-1, Mo-2, and Mo-3. The first one, Mo-1, centered at 228.1 eV, can be attributed to Mo in the non-exfoliated Mo_2Ga_2C observed in the XRD patterns (Fig. 2), at least for the Mo_2C sample. Indeed, this signal is the typical signature of this phase (see Figure S2 and related explanation). The intensity of the Mo-1 peak increases drastically for Ru/Mo_2C sample (Fig. 4). Thus, this contribution is not only due to the remaining MAX phase since the amounts of remaining gallium is close in both samples (Table 1 and S1). The increase in the Mo-1 peak intensity after ruthenium addition can be explained by the thermal treatment under H_2 at 400 °C: the partial removal of some terminal group leads to the formation of carbidic Mo, *i.e* surface Mo species not linked to terminal groups, for which the signature is at ≈228.3 eV [19]. Indeed, as observed in Figure S1, the fluorine terminal groups observed on Mo_2C (initially 0.24 F per 2 Mo, calculated by combining Tables S1 and S2 data) are fully removed in Ru/Mo_2C. Note that the re-population of the MXene surface by terminal groups during handling under air is expected. However, the duration of the exposure of the sample to air was less than 30 min (experimental part). As detailed in the supplementary information file (Figure S3 and related discussion), the re-population of the MXene surface is then very limited during this short period under air. The Mo-2 peak at ≈ 229.1 eV is undoubtedly ascribed to molybdenium sandwiched between a C layer

and a T_x adlayer [36], exhibiting an oxidation state near IV [13,19]. The attribution for Mo-3 at ≈ 232.3 eV is more questionable. In a previous study, this signal was attributed to MoO_x impurities [36], but Fedorov and co-workers associated it with Mo^{5+} at the surface of the MXene [13, 19]. Potentially, it could be a combination of both attributions since they are compatible. As observed, this contribution increases in Ru/Mo_2C (Fig. 4 and Tables S2 and S3). This can be explained by the sample preparation method. Indeed, the impregnation of ruthenium is performed in an aqueous solution and a partial oxidation of the MXene surface is possible (MXene is known to be sensitive to oxidation in water). Generated oxidized Mo surface species, potentially reduced during thermal treatment under H_2, are expected to be re-oxidized in contact with air after the treatment.

Several contributions are observed in the C 1 s region for the Mo_2C sample (Fig. 4). Most of them are attributed to the surface contamination (adventitious carbon) by exposure to ambient atmosphere (C-C, C-O, C═O), whereas the one at lowest BE, *i. e.* 283.0 eV, corresponds to C atoms bounded to Mo atoms in the MXene [36]. These contributions are also observed on Ru/Mo_2C, although they are combined with the contributions of metallic ruthenium (Ru 3d). Interestingly, 0.4 Ru per 2 Mo is obtained by quantification using Tables S1 and S3, whereas 0.05 Ru per 2 Mo is obtained by ICP analysis (Table 1). This difference between the surface analysis (XPS) and the bulk analysis (ICP) indicates clearly that the ruthenium nanoparticles are mainly on the Mo_2C surface (with low dispersion according to TEM analyses, see above).

3.2. Ammonia synthesis under continuous N_2+H_2 flow

3.2.1. Catalytic performances

The catalytic activities of Mo_2C, Ru/Mo_2C, and Mo_2Ga_2C samples were measured at 400 °C, 450 °C, and 500 °C consecutively, between 1 and 5 bar for each temperature. The obtained ammonia production rates are presented in Fig. 5.

Firstly, all studied samples are poorly active at 400 °C and atmospheric pressure, with ammonia production rates between 0.01 and 0.02 mmol h^{-1} g^{-1} (outlet NH_3 concentration: 10–15 ppm). A significant beneficial effect of the pressure is observed for all samples. Mo_2C and Ru/Mo_2C show the highest activities, with an ammonia production rate of 0.28–0.29 mmol h^{-1} g^{-1} at 400 °C and 5 bar. Compared with the tests performed at atmospheric pressure, the activity of Mo_2C is higher by approximately 10 and 20 times at 3 bar and 5 bar, respectively, and by 7 and 13 for Ru/Mo_2C. Remarkably, both Mo_2C and Ru/Mo_2C catalysts exhibit similar ammonia production rates, indicating that the ruthenium addition has no significant impact on the MXene phase activity in these conditions (continuous N_2 and H_2 flow, H_2:N_2 = 3:1). This is probably due to the low dispersion of Ru, as highlighted by TEM. The metallic surface accessibility is assumed to be low and ruthenium particles may also block Mo_2C active sites. Moreover, the MXene catalysts show an activity almost three times higher than that of the MAX phase at 400 °C and 5 bar (0.28 and 0.11 mmol h^{-1} g^{-1}, respectively), demonstrating the interest of this nanostructured 2D material, as suggested by recent theoretical DFT studies [10,20]. Thus, the presence of 16 mol% remaining MAX phase in the MXene (Table 1) induces an under-estimation of the MXene activity in ammonia synthesis.

Increasing the temperature to 450 °C significantly improves the ammonia production rate for all samples (Fig. 5b). Mo_2C and Ru/Mo_2C catalysts still show similar ammonia production rates (1.08 mmol h^{-1} g^{-1} and 1.02 mmol h^{-1} g^{-1} at 5 bar, respectively), while Mo_2Ga_2C MAX phase exhibits the lowest activity (0.30 mmol h^{-1} g^{-1} at 5 bar). Finally, Mo_2C and Ru/Mo_2C catalysts remain the most active samples at 500 °C (2.07 mmol h^{-1} g^{-1} and 1.82 mmol h^{-1} g^{-1}, respectively, at 5 bar, Fig. 5c). As previously discussed, the slight drop in NH_3 synthesis activity in the presence of Ru can be interpreted by (i) the low dispersion of ruthenium particles limiting the amount of active Ru species and (ii) the fact that Ru probably limits the accessibility to the MXene active sites.

The reproducibility and the effect of time on stream are detailed in the supplementary information file (Section 4, Figures S5 and S6).The evaluated catalysts show satisfactory stability after several hours under time on stream.

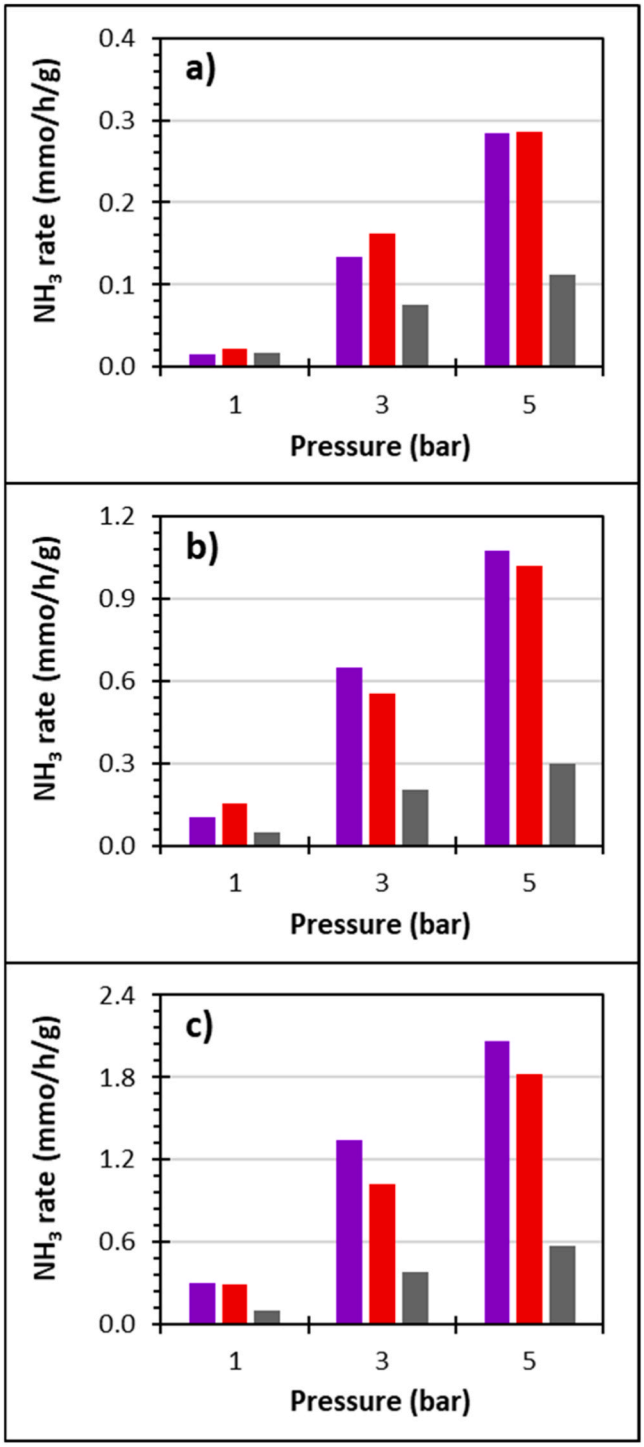

Fig. 5. Ammonia production rate (mmol h^{-1} g^{-1}) depending on the applied pressure on (■) Mo_2C, (■) Ru/Mo_2C, and (■) Mo_2Ga_2C at a) 400°C, b) 450°C and c) 500°C (color printing required).

To summarize, the activity of Mo_2C MXene in ammonia synthesis reaction varies from 0.01 mmol h^{-1} g^{-1} at 400 °C and 1 bar to 2.07 mmol h^{-1} g^{-1} at 500 °C and 5 bar. These performances are inferior to a reference Ru/MgO catalyst, previously evaluated in the same setup and conditions (3.25 mmol h^{-1} g^{-1} at 400 °C, 5 bar) [40]. Unexpectedly, it is worth noting that ammonia can be obtained with the MXene

catalyst at low pressure without ruthenium. Conversely, the presence of this metal is essential for the MgO basic oxide to produce NH_3.

This result suggests that this Mo_2C catalyst without (noble-) metallic phase is active in breaking the triple bond of molecular nitrogen (dissociative pathway). To determine if it is this type of mechanism, nitrogen homomolecular exchange was performed on Mo_2C catalyst. This method, in which a mixture of labelled nitrogen molecules, typically $^{15}N_2$ and $^{14}N_2$, is scrambled over a surface, is a powerful tool to evaluate the ability of a solid for N_2 dissociation as already described in previous reported studies [41,42]. The result (Figure S10) and related discussion are reported Section 5 of the supplementary information file and show that the homomolecular exchange reaction does not take place at 400 °C nor with increasing temperature up to 600 °C. This result makes the occurrence of a dissociative mechanism unlikely for this sample. An alternative hypothesis is that NH_3 synthesis on MXene-based catalysts follows an associative mechanism, in which successive hydrogenations of N species occur prior to dissociation of the N≡N bond. It should be noted that both mechanisms are in line with the proposal of Gouveia *et al.* [10], who showed that N_2 activation on these materials is due to the elongation of the N≡N bond. Regardless, the activity observed on noble metal-free MXene materials remains a remarkable result that opens new avenues for the development of tailored catalysts for the ammonia synthesis reaction. The following prospects for improvement need to be explored:

(i) The present work is focused on multi-layer MXenes. Previous works have shown that the accessibility of active sites for heterogeneous catalysis with MXene can be highly improved using a delaminated MXene dispersed on an inert support with a high specific surface area, such as SiO_2, to maximize the use of the 2D character of MXene [15,17].

(ii) Processing the ruthenium deposition in a colloidal suspension of delaminated MXene should improve the metal dispersion. Performed ruthenium impregnation method appears poorly efficient in the present study, as highlighted by TEM and XPS analyses. The improvement of the Ru dispersion on the MXene phase should uncover a possible role of the metallic phase used as a co-catalyst to MXene. Previous works have shown that the use of delaminated MXene is required to obtain a good dispersion of another phase [15,43], even getting single atoms [17].

(iii) Previous works have shown the primary role of a reducing thermal treatment on Mo_2CT_x activity. Modifying the T group concentration and carbon vacancies influence various reactions such as Fischer-Tropsch [19], CO_2 hydrogenation [14], or dry reforming of methane [16]. For each kind of reaction, the optimum treatment has to be adjusted (hydrogen concentration, temperature…) to obtain the best activity. In the present work, MXene was not previously pre-treated under hydrogen, even if the ammonia synthesis was performed under a H_2:N_2 (3:1) mixture. However, the pre-treatment of the catalyst needs to be studied carefully.

3.2.2. Carbon balance

The material activation process during the temperature rise was also monitored. In addition to the previously discussed ammonia production, some methane emission is observed during the temperature rise from room temperature to 400 °C (first catalytic test temperature) under the reaction flow (Fig. 6). Note that methane emission during the subsequent catalytic tests from 400 °C to 500 °C are lower than 5 ppm, and no other products are detected during the catalytic tests. Therefore, only methane emission during the initial temperature increase is discussed here. For all samples, the CH_4 production starts before the onset of NH_3 production. For Mo_2Ga_2C sample, the methane emission until 400 °C correspond to 8 $\mu mol_{CH4}\ g^{-1}$. A higher quantity of 31 $\mu mol_{CH4}\ g^{-1}$ is emitted with Mo_2C MXene phase, with an onset temperature of only 122 °C. Ruthenium addition (Ru/Mo_2C) promotes both the onset

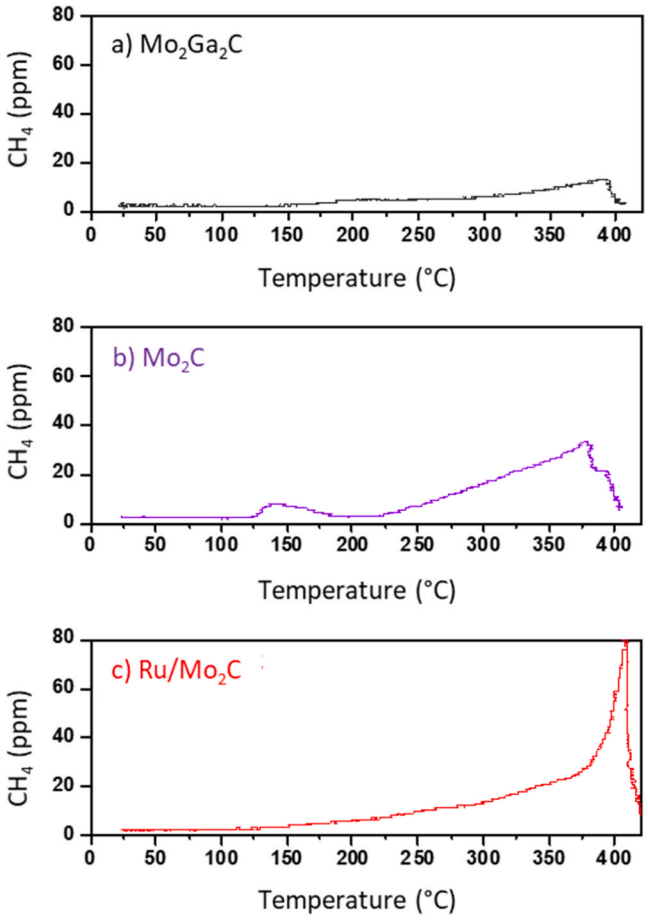

Fig. 6. CH_4 emission during the heating step from room temperature to 400 °C under the reactional mixture on (a) Mo_2Ga_2C; (b) Mo_2C; (c) Ru/Mo_2C.

temperature (100 °C) and the amount of emitted CH_4 (38 $\mu mol_{CH4}.g^{-1}$). Note that the quantity of CH_4 formed during the temperature ramp-up represents approximately 0.75 % of the carbon initially present in the Mo_2C and 1.05 % for Ru/Mo_2C (calculations performed using the $Mo_2Ga_xC_yRu_z$ formulae reported in Table 1). As a result, Ru addition does not significantly impact the carbon release mechanism. Note that this value is close to 0.3 % for Mo_2Ga_2C. In accordance with these low relative carbon losses, the CHNS elemental analysis performed before and after the catalytic tests revealed no significant carbon loss. However, since no carbonaceous compound was introduced in the gas phase, this CH_4 emission suggests that carbon from the catalysts reacts with H_2, as already observed in the literature under pure H_2 and higher temperature [19]. Thus, the material could become carbon-deficient and/or undergo nitriding due to the nitrogen in the reaction mixture (H_2:N_2 = 3:1). As previously mentioned, the nitriding could open up new avenues based on the chemical looping ammonia synthesis process, for instance. The next section is then dedicated to the study of the nitriding of the studied ($Ru/$)Mo_2C samples and possibly their reactivity toward hydrogen.

3.3. Nitriding of ($Ru/$)Mo_2C and reactivity of nitrided Mo_2C samples

The nitriding of Mo_2C MXene has already been reported through heat treatment in ammonia [32]. As mentioned in the experimental section, studied ($Ru/$)Mo_2C samples were submitted 5 hours at 600 °C, 5 bar either to 25 % NH_3 −75 % He mixture (samples denoted ($Ru/$)Mo_2C_{NH3}) or to pure N_2 (samples denoted ($Ru/$)Mo_2C_{N2}). A purge under argon at 600°C was thereafter performed. In addition, possible nitriding during catalytic tests under $N_2 + H_2$ flow was also investigated. The notation of

the corresponding samples after the catalytic tests is (Ru/)Mo_2C_{test}.

3.3.1. Characterization of the nitrided samples

The diffractograms of Mo_2C catalyst before and after the various nitriding treatments are reported in Fig. 7a. Compared to the fresh sample, a shift in the peaks of the MXene towards higher angles is observed for all materials after the thermal treatment. The c lattice parameter decreases from 20.5 Å for the fresh Mo_2C to 15.6–16 Å for the other materials, due to the removal of inter-layer water. On the contrary, the Ru/Mo_2C catalyst does not show a shift in the MXene peaks (Fig. 7b). All peaks of the MXene phase are positioned at the same angles, with c lattice parameters of 15.4–15.5 Å. Indeed, it is assumed that the removal of inter-layer water already occurs during the thermal treatment under hydrogen after ruthenium impregnation.

The elemental analysis of the catalysts was performed using both ICP-OES and CHNS analyses. The obtained formulations normalized for 2 Mo are presented in Table 2, depending on the various applied treatments. First, as expected, no significant change in the gallium content is observed, and no trace of nitrogen was detected in the "fresh" samples. Analysis after the catalytic test ((Ru/)Mo_2C_{test}) showed that the nitrogen content was very low, which does not imply a substantial nitriding of the MXene. In these conditions (400–500 °C), Ru did not influence the material's nitriding. These results support the hypothesis of an associative mechanism for NH_3 synthesis in the HB process on MXene, as discussed above. However, the possibility of MXene nitriding under reaction cannot be ruled out, since the presence of H_2 in the reactant mixture might hinder the stabilization of the intermediate nitride phase.

To the opposite, nitriding processes at a high temperature (600 °C, 5 bar, 5 h) lead to different results. For the two samples treated under NH_3 (Mo_2C_{NH3} and Ru/Mo_2C_{NH3}), close amounts of nitrogen are detected, corresponding to $N_{0.30}$ and $N_{0.24}$ stoichiometry, respectively. Thus, the thermal treatment under ammonia lead to a partial nitriding of the MXene, with no significant effect of the presence of ruthenium. Contrary to the work of Urbankowski *et al.* [32], the total nitriding of the MXene is not obtained. Two reasons can account for these differences: (i) in our work, diluted NH_3 is used contrary to pure NH_3 and (ii) the nitriding is here performed on multi-layer MXenes while a film of delaminated Mo_2CT_x sheets is used in the work of Urbankowski *et al.* [32], potentially promoting the NH_3 diffusion throughout the sample.

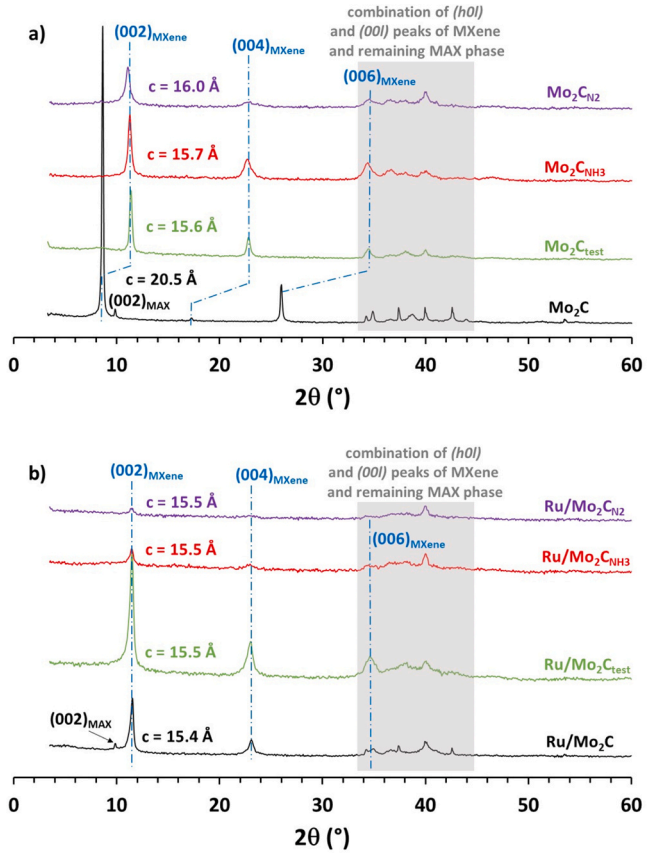

Fig. 7. Diffractograms of a) Mo_2C and b) $Ru_{2,2}/Mo_2C$ depending on the applied treatment: as prepared, after the consecutive catalytic tests at 400 °C, 450 °C and 500 °C ((Ru/)Mo_2C_{test}), after nitriding treatment under NH_3 (600°C, 1 h; (Ru/)Mo_2C_{NH3}) and after nitriding treatment under N_2 (600°C, 1 h; (Ru/)Mo_2C_{N2}).

Table 2
Material composition from ICP and CHNS analyses or XPS experiments depending on the applied thermal treatment (NH_3 600°C 5 bar; N_2 600°C 5 bar; catalytic test). The obtained formulation is normalized for 2 Mo.

sample	Chemical formulae normalized for Mo_2 from ICP and CHNS analyses						
	Mo	Ga	C	N	O	F	Ru
Mo_2C	2.00	0.30	0.91	0.00	-	-	0.00
Mo_2C_{test}	2.00	0.31	0.98	0.02	-	-	0.00
Mo_2C_{NH3}	2.00	0.34	0.89	0.30	-	-	0.00
Mo_2C_{N2}	2.00	0.33	0.89	0.03	-	-	0.00
Ru/Mo_2C	2.00	0.29	0.82	0.00	-	-	0.05
Ru/Mo_2C_{test}	2.00	0.28	1.00	0.02	-	-	0.06
Ru/Mo_2C_{NH3}	2.00	0.34	0.82	0.24	-	-	0.05
Ru/Mo_2C_{N2}	2.00	0.35	0.74	0.17	-	-	0.05
	Chemical formulae normalized for Mo_2 from XPS experiments						
Mo_2C	2.00	0.03	1.30	0.00	2.02	0.24	-
Mo_2C_{NH3}	2.00	0.06	0.90	0.40	1.61	0	-

After a treatment under pure N_2, only the sample containing ruthenium leads to a significant nitriding of Mo_2C, to a lower extent than under NH_3. The obtained stoichiometries for 2 Mo are $N_{0.17}$ and $N_{0.03}$ for Ru/Mo_2C_{N2} and Mo_2C_{N2}, respectively. The activity of ruthenium in N_2 dissociation would thus allow the nitriding of the MXene during the treatment under nitrogen flow at high temperature. Finally, note that the evolution of the carbon content determined by CHNS analysis appears not fully related to the nitrogen content and remains unclear at this stage.

Additionally, the scanning electron microscopy images coupled with EDX mapping of Mo_2C treated under NH_3 at 600 °C show that N-species are homogeneously present in the material, as for Mo and C species (Fig. 8). The EDX spectrum and the Ga EDX mapping reported in Figure S6 indicate the presence of the remaining MAX phase, in accordance with ICP analyses. Based on the mean values for atomic contents obtained by combining several EDX spectra, a composition of 0.46 N for 2 Mo is obtained (Figure S6; note that this result is approximate due to the difficulty in accurately quantifying light elements by EDX, such as N).

To investigate the nitriding, some of these materials were also studied by Raman spectroscopy and X-ray Photoelectron Spectroscopy (XPS). Although Raman spectroscopy does not clearly show sample nitriding (SI part 3), XPS does. After thermal treatment under diluted NH_3 at 600 °C and 5 bar, the Mo_2C_{NH3} sample does not exhibit significant changes in the C 1 s (Fig. 4) and O 1 s (Figure S1) regions compared to fresh Mo_2C. The same contributions are observed. Only the fluorine terminal groups are removed during the thermal treatment (Figure S2). In the Mo 3d region, no new contribution is observed after nitriding, although the intensity of the Mo-1 contribution increases compared to Mo_2C (Fig. 4). As for Ru/Mo_2C, the increase in this contribution is probably due to the partial removal of the terminal groups under reducing thermal treatment (see above). However, no difference could be observed since the characteristic bands of C-Mo-T_x are identical to those of N-Mo-T_x in the Mo 3d region, even if the MXene is fully nitrided [32,44]. The Mo 3p and N 1 s regions (in the same range of BE) were analysed to highlight possible differences indicating the presence of

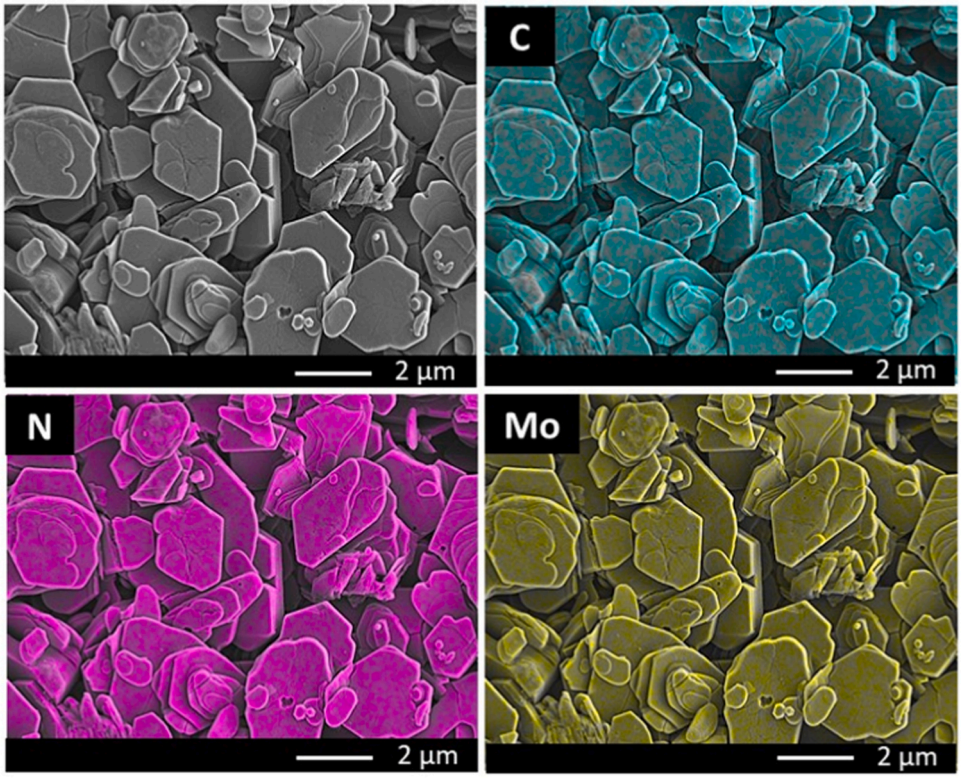

Fig. 8. Scanning electron microscopy images with EDX mapping analysis of Mo, N, and C in Mo_2C_{NH3} (color printing required).

nitrides (Fig. 9 and table S5). Indeed, a new contribution, labelled N-Mo, is required in Mo_2C_{NH3} sample at 397.6 eV to fit the experimental spectrum. This contribution is related to nitrogen atoms bonded to molybdenum atoms (nitride) according to the work of Urbankowski *et al.* (397.5 eV) [32]. The presence of this contribution is discussed in depth in the XPS section of the supplementary information file (XPS on Mo_2C_{NH3}, Figures S4 and S5). NH_x species, with peaks mainly observed between 400 and 402 eV [45,46], are not observed, in accordance with the work of Urbankowski *et al.* [32]. The purge under argon after the nitriding treatment allows the removal of these adsorbed species. Finally, these results confirm the formation of a molybdenum carbonitride phase. Then, the partial nitriding of the sample appears confirmed, in accordance with the CHNS elemental analysis.

A quantitative analysis based on the previous assignments is also performed using the results reported in Tables S1, S2, and S4 (only the contributions attributed to MXene, highlighted in red, are considered). The normalized quantification for two molybdenum atoms is presented in Table 2. Although this type of quantification is considered as semi-quantitative due to measurement uncertainties, overlapping contributions, and difficulties in attribution [35,36,47], several insights can be obtained. In Mo_2C, the obtained Mo/C ratio is close to the expected one. However, contrary to the results based on the combination of ICP and CHNS analyses, an over-stoichiometry of carbon is obtained (1.3 C for 2 Mo). Since XPS probes only the 2–4 up-layers of the multi-layer MXene, it could be due to a difference at the extreme surface by the presence of Mo vacancies formed during the etching step, sometimes observed in MXenes [36]. After the thermal treatment under NH_3, a decrease in the proportion of carbon along with an increase in the amount of nitrogen is observed, which confirms the nitriding of Mo_2C. Moreover, the C + N content (1.3) in Mo_2C_{NH3} is equivalent to the C content in Mo_2C (1.3). It

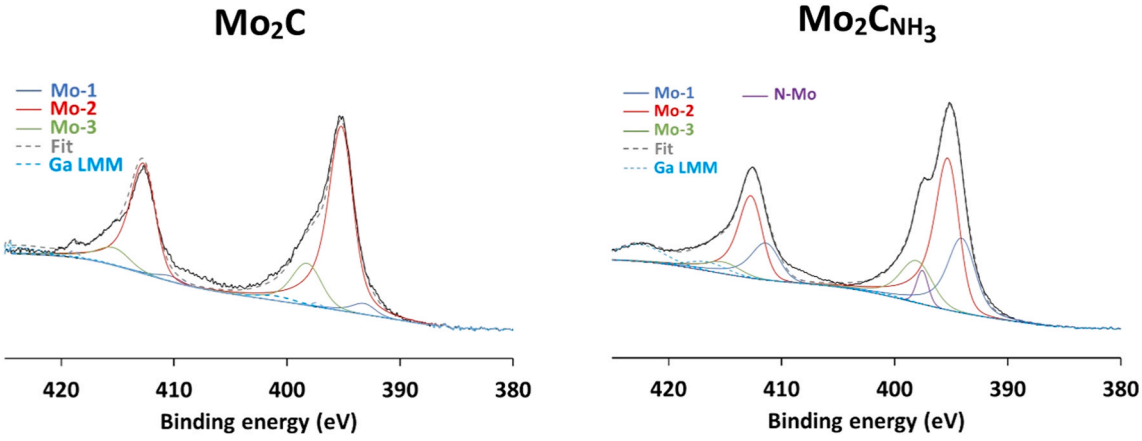

Fig. 9. High resolution XPS spectra with curve fitting of Mo 3p and N 1 s regions recorded on Mo_2C and Mo_2C_{NH3}. All spectra are normalized to the most intense peak (color printing required).

is then suggested that the nitrogen atoms take the place of the carbon in the MXene structure as proposed in the literature [32]. Finally, the N and C content are close for Mo_2C_{NH3} sample disregard of the method of quantification.

Based on theoretical DFT calculations, it is generally accepted that the number of terminal groups, including -O, -OH and -F groups, cannot exceed 2 on Mo_2CT_x MXenes, when the most stable site for them is totally occupied [48]. However, I. Persson *et al.* showed the possibility to exceed this number in specific conditions [49]. In the present study, the obtained stoichiometry is x = 2.26 for Mo_2CT_x (Table 2) but the applied method neglects the oxygens that may come from contamination impurities or molybdenum oxides (BE close to the one of C-Mo-O_x). Therefore, the exact content of terminal group cannot be assessed, only a direct comparison between Mo_2C and Mo_2C_{NH3} can be done. Indeed the obtained x coefficent decreased from 2.26 for Mo_2C to 1.61 for Mo_2C_{NH3} (Table 2). It clearly confirms that the terminal groups are partially removed, in accordance with the increase of the Mo-1 contribution in the Mo 3d region (Fig. 4).

In conclusion, this XPS study confirms the partial MXene nitriding under NH_3 with the formation of a $Mo_2C_{1-x}N_x$ nitride phase without the presence of NH_x species, probably removed during the purge under argon. Moreover, the nitriding treatment involves the partial removal of the terminal groups.

3.3.2. *Reactivity of Mo_2C nitride samples*

In this section, the reactivity of nitrogen species of $Mo_2C_{1-x}N_x$ to form ammonia is examined. With this aim, the samples (Mo_2C or Ru/Mo_2C) were pre-treated for 5 h under 25 % NH_3-75 %He (60 mL.min^{-1}) at 600 °C and 5 bar, as in the previous section to form Mo_2C_{NH3} and Ru/Mo_2C_{NH3} respectively. After a purge under argon at the same temperature and pressure for 2 h (allowing the removal of NH_x species), the sample was cooled down to room temperature and then submitted to a pure H_2 flow (60 mL.min^{-1}, 1 bar) up to 600 °C (heating rate: 5 °C min^{-1}). This temperature was maintained until NH_3 was no longer detected. The recorded outlet ammonia concentration under H_2 flow is presented in Fig. 10.

For both Mo_2C_{NH3} and Ru/Mo_2C_{NH3} MXene samples, significant amounts of ammonia are produced after a nitriding treatment under ammonia (and purge under Ar). Mo_2C_{NH3} shows a main emission peak centred at 320 °C and two other contribution at 400 °C and 480 °C, while Ru/Mo_2C_{NH3} shows only a main peak at 320 °C. This result suggests the presence of different active sites for these two materials. At this stage, we have no information to explain these differences, but potentially, during the initial step of nitriding under NH_3, the presence of Ru at the MXene surface prevents the nitriding of sites that forms NH_3 at higher temperature in the case of Mo_2C_{NH3} (possibly, basal plane *vs* edge sites). Integration of the profiles until 600 °C indicates that ammonia emission was higher with Mo_2C_{NH3} (780 μmol.g^{-1}) compared to Ru/Mo_2C_{NH3} (520 μmol.g^{-1}). Therefore, the addition of ruthenium does not increase the amount of available nitrogen in the material, in accordance with results reported in Table 2 showing a higher N content for Mo_2C_{NH3} compared to Ru/Mo_2C_{NH3}. However, the onset temperature for ammonia production is lowered by the presence of ruthenium, from 240 °C with Mo_2C_{NH3} to 210 °C with Ru/Mo_2C_{NH3}. It should be noted that in both cases, these temperatures for ammonia synthesis are remarkably low. Note that switching hydrogen for argon induced no significant ammonia emission during the heating step after nitriding. Then, the recorded ammonia production only comes from H_2 reaction with nitrogen stored in the material. This reactivity of lattice nitrogen to form ammonia under H_2 was already observed on conventional 3D MoC_xN_y carbonitrides by Alshalwi *et al.* [50].

3.3.3. *Nitriding–H_2 cycling tests*

Since previous results show that nitrogen stored in the MXene can subsequently be utilized to form ammonia, several successive nitriding and reaction under H_2 were performed to investigate the feasibility of a cycled ammonia production process (close to the chemical looping concept). For this experiment, Mo_2C nitrided with NH_3 was selected even if nitriding under ammonia has no economic sense to produce ammonia by chemical looping. However, this treatment allows a better nitriding efficiency (Table 2) with the aim to evaluate the concept. Experimentally, the catalyst was first heated under argon until 600 °C (5 °C min^{-1}). At this temperature, nitriding was then carried out under 25 % NH_3–75 % He (10 mL min^{-1}, 5 bar, 30 minutes). After a purge under argon (60 mL min^{-1}, 5 bar) until the NH_3 concentration reached the baseline, the sample was submitted to a H_2 flow (60 mL min^{-1}, 5 bar). The concentration profiles of ammonia and methane recorded with Mo_2C sample during the steps under hydrogen for consecutive cycles are reported in Fig. 11.

As expected, during the first hydrogen period after nitriding, a significant amount of ammonia is produced, representing 770 μmol g^{-1} of NH_3. In successive cycles, ammonia is also observed under H_2 flow, indicating that MXene multiple consecutive nitriding is possible. During the second cycle, the ammonia emission decreases to 330 μmol g^{-1}. In subsequent

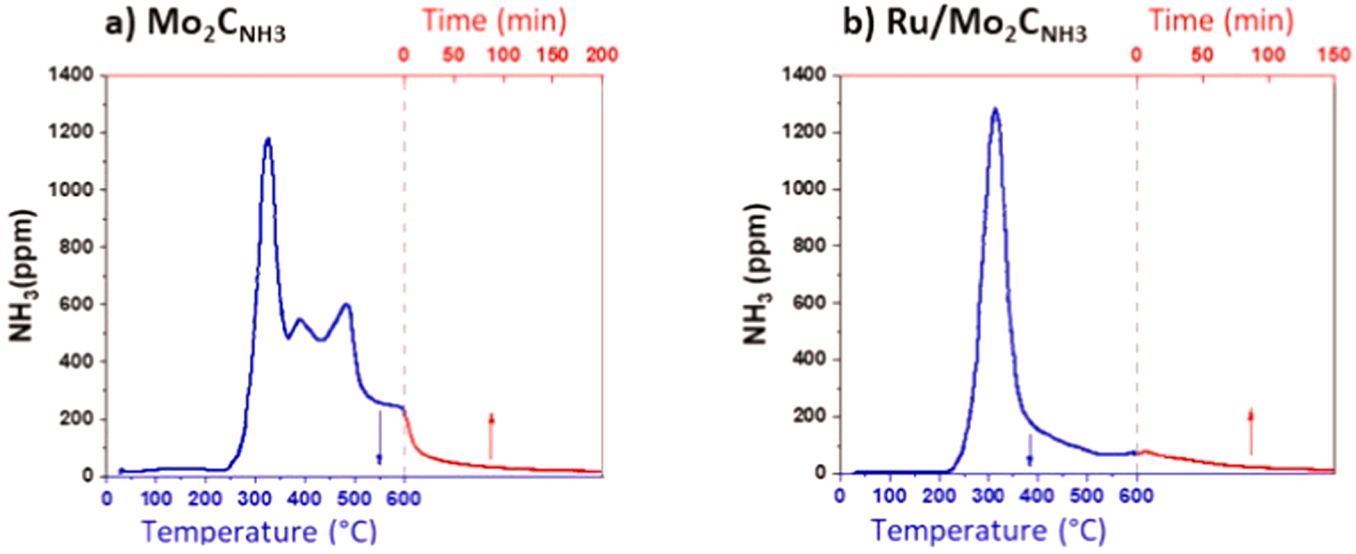

Fig. 10. Ammonia outlet profiles under pure H_2 flow with a) Mo_2C_{NH3} and b) Ru/Mo_2C_{NH3}, both after nitriding with NH_3 at 600°C and purge under Ar (all steps of the test were performed at 5 bar).

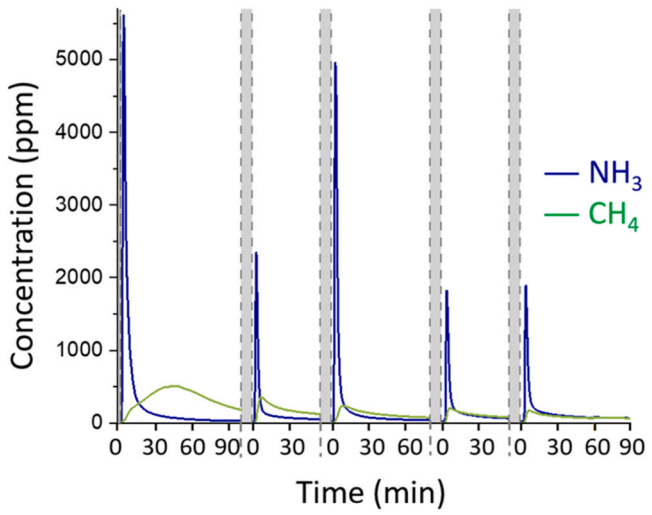

Fig. 11. NH_3 and CH_4 outlet concentrations recorded with Mo_2C sample during the steps under hydrogen flow (600 °C et 5 bar) after nitriding treatments under NH_3 at 600 °C and 5 bar (grey zones represent the intermediate nitriding treatment) (color printing required).

cycles, the ammonia emission tends to stabilisation around 300 μmol g^{-1}. Methane is simultaneously detected with a progressive decrease in its concentration over successive cycles. The total amount of methane emission after the five step under hydrogen represents 1960 μmol g^{-1}, which is half of the amount of carbon present in the initial catalyst.

Based on the previous XPS study (Section 3.3.1) and the literature data [32], it is clear that a carbonitride is obtained by nitriding under NH_3. This is confirmed by the carbon removal under cycling (CH_4 formation) due to the progressive replacement of C by N in the MXene structure. No trace of NH_x was detected by XPS on the carbonitride samples (see above), indicating that the purge under argon at 600 °C after the nitriding step allows the removal of NH_x species. By considering a maximum of 0.3 N for 2 Mo after the first nitriding cycle during 30 min (value obtained after nitriding for 6 h in the same conditions – Table 2), the ammonia formation (770 μmol g^{-1}) corresponds to at least 67 % of the initial N content in the material. Consequently, the possibility that ammonia was formed mostly from remaining NH_x species is excluded because such quantities would have been detected by XPS. Therefore, it appears feasible to cyclically use the molybdenum carbonitride phase ($Mo_2C_{1-x}N_x$) for ammonia production.

Finally, the production of ammonia by a direct reaction of the nitrided Mo_2C MXene material with H_2 (in the absence of N_2) is clearly evidenced (Figs. 10 and 11). Such a behaviour was reported on more classical carbide materials in particular by Hargreaves and co-workers [51,52] but, to our knowledge, it was never experimentally demonstrated on MXenes. Therefore, it paves the way for the utilization of MXene in the chemical looping ammonia synthesis (CLAS) process if the regeneration of the nitride phase can occur under N_2. On Ru/Mo_2C, this step occurs at 600 °C but with slow kinetics. Again, the slow kinetics could potentially be enhanced by improving the Ru dispersion on delaminated MXene.

4. Conclusion

This study investigated Mo_2C (MXene) performances for ammonia thermocatalytic synthesis. Under a H_2-N_2 flow, Mo_2C MXene phase showed limited activity in ammonia synthesis at atmospheric pressure at 400 °C (0.01 mmol h^{-1} g^{-1}), but it increased significantly with temperature and pressure, to 2.07 mmol h^{-1} g^{-1} at 500 °C and 5 bar. Interestingly, the MXene is active without Ru additive, which possibly indicates an associative mechanism. Unexpectedly, the addition of ruthenium did not enhance the activity of the Mo_2C MXene catalyst in our conditions. In addition, methane formation was also observed during the heating step, while ammonia production did not occur yet. This methane formation could be associated with the nitriding of the material and/or the partial removal of carbon under reducing conditions. For this reaction, ruthenium promotes both the onset temperature (100 °C) and the amount of emitted CH_4 until 400 °C. This study highlighted various ways (dispersion of delaminated MXene on a support, conditions of activation, dispersion of Ru…) for future works to improve the performances of the MXene toward the Haber-Bosch process. Moreover, the chemical richness of the MXene family could be also explore in future works to improve their performances toward the HB process, especially W_2C, known as promising catalyst for this reaction based on DFT studies**.** Additionally, since (carbo)nitrides can be obtained from Mo_2C MXene phase as showed in this work, investigation of the behaviors of such compounds deserves particular attention.

Beside, Mo_2CT_x MXene has shown potential for the chemical looping process. Thermal treatment under NH_3 (600 °C, 5 bar) was found to be the most efficient route for nitriding the MXene toward the formation of a carbonitride. Interestingly, in the presence of ruthenium, nitriding can also occur under N_2 (600 °C, 5 bar), in a lower extent compared with NH_3. This behaviour is probably related to the ruthenium ability toward the N≡N triple bond cleavage. The reactivity of incorporated nitrogen in the MXene phase was also evaluated under hydrogen flow (5 bar). In this case, ammonia emission started at very low temperature, lower than 250 °C. Moreover, it was found that storing nitrogen compounds and then forming ammonia under pure hydrogen flow was consecutively repeatable for 5 cycles, similarly to the chemical looping ammonia synthesis process. However, in this alternative concept that aims to overcome kinetic and thermodynamic limitations, it appears necessary to perform the nitriding step under N_2 rather than NH_3. With this aim, the optimization of the ruthenium deposition at the MXene surface remains an attractive way.

Additionally, delamination of the MXene could potentially increase the catalytic activity of the material, enabling a deposition on a support with a higher specific surface area to disperse the MXene layers. As supported, delaminated MXene could also facilitate the dispersion of ruthenium, allowing a better evaluation of the metal influence in interaction with the MXene. A well-dispersed MXene could favour also the rate of nitriding by increasing the interaction of the MXene surface with N_2.

CRediT authorship contribution statement

Fabien Can: Writing – review & editing, Supervision, Methodology, Investigation, Funding acquisition, Formal analysis, Data curation, Conceptualization. **Nicolas Bion:** Supervision, Methodology, Investigation, Funding acquisition, Formal analysis, Conceptualization. **Julie Rousseau:** Formal analysis. **Christine Canaff:** Investigation, Formal analysis. **Lola Loupias:** Investigation, Formal analysis. **stéphane célérier:** Writing – review & editing, Supervision, Investigation, Funding acquisition, Formal analysis, Data curation. **Xavier Courtois:** Writing – review & editing, Supervision, Methodology, Investigation, Formal analysis, Data curation, Conceptualization. **Charlotte Croisé:** Writing – original draft, Methodology, Investigation, Formal analysis, Conceptualization.

Declaration of Competing Interest

The authors declare the following financial interests/personal relationships which may be considered as potential competing interests: Celerier reports financial support was provided by French National Research Agency. Can reports financial support was provided by French National Research Agency. If there are other authors, they declare that they have no known competing financial interests or personal relationships that could have appeared to influence the work reported in this paper.

Acknowledgements

The authors gratefully acknowledge the French National Agency for Research (ANR, Intermetalyst Project, ref. ANR-19-CE07–0023 and MXENECAT project, ref ANR-18-CE08–014), the Regional Council of Nouvelle Aquitaine (Néo-Ammonia project, AAPR2020–2019–8018010), the French Ministry of Research and the European Regional Development Fund (ERDF) for financial supports. This work also pertains to the French government program "Investissements d'Avenir" (EUR INTREE, reference ANR-18-EURE-0010). The authors wish to thanks S. Arrii for XRD experiments, N. Guignard for Raman and P. Chartier for the MAX phase synthesis.

Appendix A. Supporting information

Supplementary data associated with this article can be found in the online version at doi:10.1016/j.mtcata.2024.100066.

References

[1] Irena, A.E.A., Innovation Outlook: Renewable Ammonia, International Renewable Energy Agency, Abu Dhabi, Ammonia Energy Association, Brooklyn., 2022. ⟨https://research.utwente.nl/en/publications/innovation-outlook-renewable-ammonia⟩.
[2] A.I. Amhamed, S. Shuibul Qarnain, S. Hewlett, A. Sodiq, Y. Abdellatif, R.J. Isaifan, O.F. Alrebei, Ammonia production plants—a review, Fuels 3 (2022) 408–435, https://doi.org/10.3390/fuels3030026.
[3] A. Valera-Medina, H. Xiao, M. Owen-Jones, W.I.F. David, P.J. Bowen, Ammonia for power, Prog. Energy Combust. Sci. 69 (2018) 63–102, https://doi.org/10.1016/j.pecs.2018.07.001.
[4] H. Liu, Ammonia synthesis catalyst 100 years: Practice, enlightenment and challenge, Chin. J. Catal. 35 (2014) 1619–1640, https://doi.org/10.1016/S1872-2067(14)60118-2.
[5] J.W. Erisman, M.A. Sutton, J. Galloway, Z. Klimont, W. Winiwarter, How a century of ammonia synthesis changed the world, Nat. Geosci. 1 (2008) 636–639, https://doi.org/10.1038/ngeo325.
[6] Ammonia Technology Roadmap – Analysis, IEA (2021). ⟨https://www.iea.org/reports/ammonia-technology-roadmap⟩ (accessed April 16, 2024).
[7] J. Humphreys, R. Lan, S. Tao, Development and recent progress on ammonia synthesis catalysts for haber–bosch process, Adv. Energy Sustain. Res. 2 (2021) 2000043, https://doi.org/10.1002/aesr.202000043.
[8] W. Raróg-Pilecka, E. Miśkiewicz, S. Jodzis, J. Petryk, D. Łomot, Z. Kaszkur, Z. Karpiński, Z. Kowalczyk, Carbon-supported ruthenium catalysts for NH3 synthesis doped with caesium nitrate: Activation process, working state of Cs–Ru/C, J. Catal. 239 (2006) 313–325, https://doi.org/10.1016/j.jcat.2006.01.035.
[9] Á. Morales-García, F. Calle-Vallejo, F. Illas, MXenes: new horizons in catalysis, ACS Catal. 10 (2020) 13487–13503, https://doi.org/10.1021/acscatal.0c03106.
[10] J.D. Gouveia, Á. Morales-García, F. Viñes, J.R.B. Gomes, F. Illas, Facile heterogeneously catalyzed nitrogen fixation by MXenes, ACS Catal. 10 (2020) 5049–5056, https://doi.org/10.1021/acscatal.0c00935.
[11] A. VahidMohammadi, J. Rosen, Y. Gogotsi, The world of two-dimensional carbides and nitrides (MXenes), Science 372 (2021), https://doi.org/10.1126/science.abf1581.
[12] M. Naguib, M. Kurtoglu, V. Presser, J. Lu, J. Niu, M. Heon, L. Hultman, Y. Gogotsi, M.W. Barsoum, Two-dimensional nanocrystals produced by exfoliation of Ti3AlC2, Adv. Mater. 23 (2011) 4248–4253, https://doi.org/10.1002/adma.201102306.
[13] E.B. Deeva, A. Kurlov, P.M. Abdala, D. Lebedev, S.M. Kim, C.P. Gordon, A. Tsoukalou, A. Fedorov, C.R. Müller, In Situ XANES/XRD study of the structural stability of two-dimensional molybdenum carbide Mo2CTx: implications for the catalytic activity in the water–gas shift reaction, Chem. Mater. 31 (2019) 4505–4513, https://doi.org/10.1021/acs.chemmater.9b01105.
[14] H. Zhou, Z. Chen, E. Kountoupi, A. Tsoukalou, P.M. Abdala, P. Florian, A. Fedorov, C.R. Müller, Two-dimensional molybdenum carbide 2D-Mo2C as a superior catalyst for CO2 hydrogenation, Nat. Commun. 12 (2021) 5510, https://doi.org/10.1038/s41467-021-25784-0.
[15] H. Zhou, Z. Chen, A.V. López, E.D. López, E. Lam, A. Tsoukalou, E. Willinger, D. A. Kuznetsov, D. Mance, A. Kierzkowska, F. Donat, P.M. Abdala, A. Comas-Vives, C. Copéret, A. Fedorov, C.R. Müller, Engineering the Cu/Mo2CTx (MXene) interface to drive CO2 hydrogenation to methanol, Nat. Catal. 4 (2021) 860–871, https://doi.org/10.1038/s41929-021-00684-0.
[16] A. Kurlov, E.B. Deeva, P.M. Abdala, D. Lebedev, A. Tsoukalou, A. Comas-Vives, A. Fedorov, C.R. Müller, Exploiting two-dimensional morphology of molybdenum oxycarbide to enable efficient catalytic dry reforming of methane, Nat. Commun. 11 (2020) 4920, https://doi.org/10.1038/s41467-020-18721-0.
[17] Y. Yan, D. Sall, L. Loupias, S. Célérier, M. Aouine, P. Bargiela, M. Prévot, F. Morfin, L. Piccolo, MXene-supported single-atom and nano catalysts for effective gas-phase hydrogenation reactions, Mater. Today Catal. 2 (2023) 100010, https://doi.org/10.1016/j.mtcata.2023.100010.
[18] R. Morales-Salvador, J.D. Gouveia, Á. Morales-García, F. Viñes, J.R.B. Gomes, F. Illas, Carbon capture and usage by MXenes, ACS Catal. 11 (2021) 11248–11255, https://doi.org/10.1021/acscatal.1c02663.
[19] E. Kountoupi, A.J. Barrios, Z. Chen, C.R. Müller, V.V. Ordomsky, A. Comas-Vives, A. Fedorov, The impact of oxygen surface coverage and carbidic carbon on the activity and selectivity of two-dimensional molybdenum carbide (2D-Mo2C) in Fischer–Tropsch synthesis, ACS Catal. 14 (2024) 1834–1845, https://doi.org/10.1021/acscatal.3c03956.
[20] M. Shao, Y. Shao, W. Chen, K.L. Ao, R. Tong, Q. Zhu, I.N. Chan, W.F. Ip, X. Shi, H. Pan, Efficient nitrogen fixation to ammonia on MXenes, Phys. Chem. Chem. Phys. 20 (2018) 14504–14512, https://doi.org/10.1039/C8CP01396A.
[21] M. López, Á. Morales-García, F. Viñes, F. Illas, Thermodynamics and kinetics of molecular hydrogen adsorption and dissociation on MXenes: relevance to heterogeneously catalyzed hydrogenation reactions, ACS Catal. 11 (2021) 12850–12857, https://doi.org/10.1021/acscatal.1c03150.
[22] Y. Luo, G.F. Chen, L. Ding, X. Chen, L.X. Ding, H. Wang, Efficient electrocatalytic N2 fixation with mxene under ambient conditions, Joule 3 (2019) 279–289, https://doi.org/10.1016/j.joule.2018.09.011.
[23] J. Xia, H. Guo, G. Yu, Q. Chen, Y. Liu, Q. Liu, Y. Luo, T. Li, E. Traversa, 2D Vanadium Carbide (MXene) for electrochemical synthesis of ammonia under ambient conditions, Catal. Lett. 151 (2021) 3516–3522, https://doi.org/10.1007/s10562-021-03589-6.
[24] Y. Guo, T. Wang, Q. Yang, X. Li, H. Li, Y. Wang, T. Jiao, Z. Huang, B. Dong, W. Zhang, J. Fan, C. Zhi, Highly efficient electrochemical reduction of nitrogen to ammonia on surface termination modified Ti3C2Tx MXene nanosheets, ACS Nano 14 (2020) 9089–9097, https://doi.org/10.1021/acsnano.0c04284.
[25] T. Guo, D. Zhou, C. (John) Zhang, Perspectives on electrochemical nitrogen fixation catalyzed by two-dimensional MXenes, Mater. Rep.: Energy 2 (2022) 100076, https://doi.org/10.1016/j.matre.2021.100076.
[26] Y. Gao, Y. Cao, H. Zhuo, X. Sun, Y. Gu, G. Zhuang, S. Deng, X. Zhong, Z. Wei, X. Li, J. Wang, Mo2TiC2 MXene: A Promising Catalyst for Electrocatalytic Ammonia Synthesis, Catal. Today 339 (2020) 120–126, https://doi.org/10.1016/j.cattod.2018.12.029.
[27] A.L.A. Marinho, C. Comminges, A. Habrioux, S. Célérier, N. Bion, C. Morais, Reactivity of nitrogen atoms from Zif-8 structure deposited over Ti3C2 MXene in the electrochemical nitrogen reduction reaction, Chem. Commun. 59 (2023) 10133–10136, https://doi.org/10.1039/D3CC02693K.
[28] A. Liu, X. Liang, M. Gao, X. Ren, L. Gao, Y. Yang, H. Zhu, G. Li, T. Ma, Ru and Fe Alloying on a two-dimensional MXene support for enhanced electrochemical synthesis of ammonia, ChemCatChem 14 (2022) e202101775, https://doi.org/10.1002/cctc.202101775.
[29] A. Liu, X. Liang, Q. Yang, X. Ren, M. Gao, Y. Yang, T. Ma, Electrocatalytic synthesis of ammonia using a 2D Ti3C2 MXene loaded with copper nanoparticles, ChemPlusChem 86 (2021) 166–170, https://doi.org/10.1002/cplu.202000702.
[30] F. Wang, Y. Wang, L. Li, Z. Li, W. Zhang, Z. Xue, D. Liu, X. Meng, C. Li, J. Sunarso, S. Liu, N. Yang, Electrocatalytic ammonia synthesis on Fe@MXene catalyst as cathode of intermediate-temperature proton-conducting solid oxide cell, Int. J. Hydrog. Energy 48 (2023) 17677–17688, https://doi.org/10.1016/j.ijhydene.2023.01.256.
[31] S. Brown, J. Hu, Review of chemical looping ammonia synthesis materials, Chem. Eng. Sci. 280 (2023) 119063, https://doi.org/10.1016/j.ces.2023.119063.
[32] P. Urbankowski, B. Anasori, K. Hantanasirisakul, S.J.L. Billinge, Y. Gogotsi, 2D molybdenum and vanadium nitrides synthesized by ammoniation of 2D transition metal carbides (MXenes), R. Soc. Chem. (2017) 17722–17730, https://doi.org/10.1039/c7nr06721f.
[33] M. Benchakar, V. Natu, T.A. Elmelegy, M. Sokol, J. Snyder, C. Comminges, C. Morais, S. Célérier, A. Habrioux, M.W. Barsoum, On a two-dimensional MoS2/Mo2CTx hydrogen evolution catalyst obtained by the topotactic sulfurization of Mo2CTx MXene, J. Electrochem. Soc. 167 (2020) 124507, https://doi.org/10.1149/1945-7111/abad6e.
[34] L.-Å. Näslund, I. Persson, XPS spectra curve fittings of Ti3C2Tx based on first principles thinking, Appl. Surf. Sci. 593 (2022) 153442, https://doi.org/10.1016/j.apsusc.2022.153442.
[35] M. Benchakar, L. Loupias, C. Garnero, T. Bilyk, C. Morais, C. Canaff, N. Guignard, S. Morisset, H. Pazniak, S. Hurand, P. Chartier, J. Pacaud, V. Mauchamp, M. W. Barsoum, A. Habrioux, S. Célérier, One MAX phase, different MXenes: A guideline to understand the crucial role of etching conditions on Ti3C2Tx surface chemistry, Appl. Surf. Sci. 530 (2020) 147209, https://doi.org/10.1016/j.apsusc.2020.147209.
[36] L. Loupias, C. Morais, S. Morisset, C. Canaff, Z. Li, F. Brette, P. Chartier, N. Guignard, L. Maziere, V. Mauchamp, T. Cabioc'h, A. Habrioux, S. Célérier, Guideline for synthesis and surface chemistry characterization of 2D Mo/Ti solid solutions based MXene. Application to hydrogen evolution reaction in alkaline media, FlatChem 43 (2024) 100596, https://doi.org/10.1016/j.flatc.2023.100596.
[37] J. Halim, S. Kota, M.R. Lukatskaya, M. Naguib, M.-Q. Zhao, E.J. Moon, J. Pitock, J. Nanda, S.J. May, Y. Gogotsi, M.W. Barsoum, Synthesis and characterization of 2D molybdenum carbide (MXene), Adv. Funct. Mater. 26 (2016) 3118–3127, https://doi.org/10.1002/adfm.201505328.
[38] S. Célérier, S. Hurand, C. Garnero, S. Morisset, M. Benchakar, A. Habrioux, P. Chartier, V. Mauchamp, N. Findling, B. Lanson, E. Ferrage, Hydration of Ti3C2Tx MXene: an interstratification process with major implications on physical properties, Chem. Mater. 31 (2019) 454–461, https://doi.org/10.1021/acs.chemmater.8b03976.
[39] C.J.H. Jacobsen, S. Dahl, P.L. Hansen, E. Törnqvist, L. Jensen, H. Topsøe, D.V. Prip, P.B. Møenshaug, I. Chorkendorff, Structure sensitivity of supported ruthenium catalysts for ammonia synthesis, J. Mol. Catal. A: Chem. 163 (2000) 19–26, https://doi.org/10.1016/S1381-1169(00)00396-4.
[40] C. Croisé, K. Alabd, S. Tencé, E. Gaudin, A. Villesuzanne, X. Courtois, N. Bion, F. Can, Influence of the Rare Earth (R) Element in Ru-supported RScSi Electride-

like Intermetallic Catalysts for Ammonia Synthesis at Low Pressure: Insight into NH3 Formation Mechanism, ChemCatChem 15 (2023) e202201172, https://doi.org/10.1002/cctc.202201172.
[41] C. Croisé, K. Alabd, A. Villesuzanne, F. Can, X. Courtois, E. Gaudin, S. Tencé, N. Bion, Role of hydride ion within Ru/LaScSi and Ru/CeTiGe catalysts for NH3 synthesis: A combination of DFT and experimental nitrogen isotopic exchange studies, Catal. Commun. 179 (2023) 106689, https://doi.org/10.1016/j.catcom.2023.106689.
[42] T.-N. Ye, S.-W. Park, Y. Lu, J. Li, M. Sasase, M. Kitano, H. Hosono, Contribution of nitrogen vacancies to ammonia synthesis over metal nitride catalysts, J. Am. Chem. Soc. 142 (2020) 14374–14383, https://doi.org/10.1021/jacs.0c06624.
[43] L. Loupias, R. Boulé, C. Morais, V. Mauchamp, N. Guignard, J. Rousseau, J. Pacaud, P. Chartier, M. Gaudon, C. Coutanceau, S. Célérier, A. Habrioux, Mo2CTx MXene supported nickel-iron alloy: an efficient and stable heterostructure to boost oxygen evolution reaction, 2D Mater. 10 (2023) 024005, https://doi.org/10.1088/2053-1583/acbfcb.
[44] J. Li, C. Zhou, J. Mu, E.-C. Yang, X.-J. Zhao, In situ synthesis of molybdenum carbide/N-doped carbon hybrids as an efficient hydrogen-evolution electrocatalyst, RSC Adv. 8 (2018) 17202–17208, https://doi.org/10.1039/C8RA02020E.
[45] C. Guimon, A. Zouiten, A. Boreave, G. Pfister-Guillouzo, P. Schulz, F. Fitoussi, C. Quet, Surface and subsurface acidity of faujasite-type zeolites in relation to their composition: an XPS and TPD of ammonia study, J. Chem. Soc. Faraday Trans. 90 (1994) 3461–3467, https://doi.org/10.1039/FT9949003461.
[46] R.J.J. Jansen, H. van Bekkum, XPS of nitrogen-containing functional groups on activated carbon, Carbon 33 (1995) 1021–1027, https://doi.org/10.1016/0008-6223(95)00030-H.
[47] V. Natu, M. Benchakar, C. Canaff, A. Habrioux, S. Célérier, M.W. Barsoum, A critical analysis of the X-ray photoelectron spectra of Ti3C2Tz MXenes, Matter 4 (2021) 1224–1251, https://doi.org/10.1016/j.matt.2021.01.015.
[48] F. Brette, D. Kourati, M. Paris, L. Loupias, S. Célérier, T. Cabioc'h, M. Deschamps, F. Boucher, V. Mauchamp, Assessing the surface chemistry of 2D transition metal carbides (MXenes): a combined experimental/theoretical 13C solid state NMR approach, J. Am. Chem. Soc. 145 (2023) 4003–4014, https://doi.org/10.1021/jacs.2c11290.
[49] I. Persson, J. Halim, T.W. Hansen, J.B. Wagner, V. Darakchieva, J. Palisaitis, J. Rosen, P.O.Å. Persson, How much oxygen can a MXene surface take before it breaks? Adv. Funct. Mater. 30 (2020) 1909005, https://doi.org/10.1002/adfm.201909005.
[50] M. AlShalwi, J.S.J. Hargreaves, J.J. Liggat, D. Todd, The reactivity of lattice carbon and nitrogen species in molybdenum (oxy)carbonitrides prepared by single-source routes, Mater. Res. Bull. 47 (2012) 1251–1256, https://doi.org/10.1016/j.materresbull.2012.01.022.
[51] A. Daisley, J.S.J. Hargreaves, Nitrides, hydrides and carbides as alternative heterogeneous catalysts for ammonia synthesis: a brief overview: recent approaches to nitrogen activation, Johns. Matthey Technol. Rev. 66 (2022) 326–330, https://doi.org/10.1595/205651322X16493249558666.
[52] A. Daisley, J.S.J. Hargreaves, The role of interstitial species upon the ammonia synthesis activity of ternary Fe–Mo–C(N) and Ni–Mo–C(N) phases, J. Energy Chem. 39 (2019) 170–175, https://doi.org/10.1016/j.jechem.2019.01.026.